Determination of Spatially-Distributed Hydrological Ecosystem Services (HESS) in the Red River Delta Using a Calibrated SWAT Model

Ha, Lan Thanh; Bastiaanssen, Wim G. M.

DOI
10.3390/su15076247

Publication date
2023

Document Version
Final published version

Published in
Sustainability

sustainability

MDPI

Article

Determination of Spatially-Distributed Hydrological Ecosystem Services (HESS) in the Red River Delta Using a Calibrated SWAT Model

Lan Thanh Ha [1,2,*] and Wim G. M. Bastiaanssen [1,3]

[1] Faculty of Civil Engineering and Geosciences, Delft University of Technology, 2628 CN Delft, The Netherlands
[2] Institute of Water Resources Planning, 162A Tran Quang Khai, Hanoi 100000, Vietnam
[3] IrriWatch, Agro Business Park 10, 6708 PW Wageningen, The Netherlands
* Correspondence: t.l.ha-2@tudelft.nl

Abstract: The principles of Integrated Water Resources Management (IWRM), conservation of natural capital, and water accounting requires Hydrological Eco-System Services (HESS) to be determined. This paper presents a modeling approach for quantifying the HESS framework using the Soil Water Assessment Tool (SWAT). SWAT was used–after calibration against remote sensing data–to quantify and spatially identify total runoff, natural livestock feed production, fuelwood from natural forests, dry season flow, groundwater recharge, root zone storage for carrying over water from wet to dry season, sustaining rainfall, peak flow attenuation, carbon sequestration, microclimate cooling, and meeting environmental flow requirements. The environmental value of the current land use and vegetation was made explicit by carrying out parallel simulations for bare soil and vegetation conditions and reporting the incremental ecosystem services. Geographical areas with more and fewer HESS are identified. The spatial and temporal variability of annual HESS services is demonstrated for the Day Basin—which is part of the Red River delta (Vietnam)—for the period 2003 to 2013. The result shows that even though the basin is abundant with HESS, e.g., 7482 m^3/ha of runoff, 3820 m^3/ha of groundwater recharge, the trend for many HESS values, e.g., micro-climate cooling, meeting environmental flow requirements, and rootzone storage, are declining. It is found and proven that quantified HESS indicators highlighted the provisioning and regulating characters of ecosystem services, as well as geographical hotspots across the basin. The SWAT model shows the capability of simulating terrestrial eco-hydrological processes such as climate, soil, and current land use. The methodology illustrates how eco-hydrologists can benchmark ecosystem values and include HESS in exploring river basin management scenarios, climate change studies, and land use planning.

Keywords: hydrological ecosystem services; hydrological modeling; remote sensing; ecosystem service accounting; SWAT; Red River Basin

Citation: Ha, L.T.; Bastiaanssen, W.G.M. Determination of Spatially-Distributed Hydrological Ecosystem Services (HESS) in the Red River Delta Using a Calibrated SWAT Model. *Sustainability* **2023**, *15*, 6247. https://doi.org/10.3390/su15076247

Academic Editors: Ifigenia Kagalou, Dionissis Latinopoulos and Chrysoula Ntislidou

Received: 11 February 2023
Revised: 22 March 2023
Accepted: 29 March 2023
Published: 5 April 2023

1. Introduction

Ecosystem services are defined as the benefits that people obtain from natural systems [1,2]. The concept of ecosystem services is relevant for connecting people to nature [3,4]. Hydrological Eco-System Services (HESS), also known as Water-related Ecosystem Services, comprise those ecosystem services that explicitly describe the services rendered from and regulated by water resources [5]. Because regions with local water scarcity are expanding and intensifying [6], it is becoming more important to understand and quantitatively describe the environmental benefits of water in longer-term water policy plans. Too often, multiple-use aspects of water allocation and water resources evaluation are restricted to food production, industrial use, domestic sector, and hydropower (e.g., FAO AquaStat database [7]). A HESS is less common because it is a co-product of given practices. For instance, crops are grown to generate food, not for the reduction of erosion or sequestration of carbon. Nevertheless, this co-product can be very valuable for conserving

the environment and sometimes have economic benefits such as certified carbon pools. The lacking of standardized processing and reporting of the HESS process limits the uptake by policymakers [8–10].

Based on an internationally recognized framework for Ecosystem Services and Resilience produced under the CGIAR Research Program on Water, Land, and Ecosystems [11], Ha et al., 2023 [12] described key HESS indicators that are ascribed to consumptive use and non-consumptive use. The HESS framework can be used for implementing policy frameworks such as Water Accounting [13,14].

The quantification of HESS in heterogeneous watersheds and river basins requires modeling efforts. This is especially a challenge in low-income countries such as Vietnam, where data on water resources and the environment are scarce and not easily available. Conceptually different approaches have been used for modeling, mapping, and quantifying of hydrological ecosystem services [15–19]. Quantification of these hydrological ecosystem services is based on empirically established relationships and look-up tables [20,21], hydrological-based simulation models [22], remote sensing measurements [23], or big data sets where various data sources are merged [24,25]. The main advantage of hydrological models is their great flexibility in forecasting changing conditions and assessing trade-offs if certain interventions are implemented, i.e., what is the impact of deforestation on peak flow attenuation and groundwater recharge? Some examples of modeling provisioning services are water yield, carbon stock in vegetation and soil [26], carbon fluxes [27], crop biomass production [28,29], and feed biomass production [30]. Regulating services can be described using numerical simulations of dry season base flow and groundwater recharge [31], nutrient load, sediment [32], etc.

Various types of hydrological models are suitable for modeling hydrological ecosystem services, such as SWAT [33], ARIES [34,35], INVEST [36], and VIC [37]. SWAT was recommended as a preferred tool to simulate provisioning and regulating services due to the inclusion of processes on hydrological, flow dynamics, water quality, as well as plant growth, and nutrient loading as well as in basins with no or little field measurements [38–40]. As a hydrological model, SWAT has been used at various temporal scales to simulate plot size as well as continental watersheds [41]. Its multiple input parameters and process-based biogeochemical sub-models strengthen the model's applicability to simulate not only water flow dynamics but also estimate several water quality and plant growth variables that can be used in the assessments of land and agricultural management impacts on ES. Various authors used SWAT to simulate crop growth and soil water modules [42], water and carbon fluxes [43], nutrient and sediment transport related to best management practices, wetlands, irrigation, bioenergy crops, climate change, land use change, and others [44,45].

While [12] defined a standard set of HESS indicators and pleaded for determination by means of earth observation data, not all of them can be determined from remote sensing measurements. Certain hydrological processes, such as base flow, environmental flow, and peak flow mitigation, need to be derived from a hydrological model. [46] showed how SWAT and SWAT-CUP could be employed to calibrate key eco-hydrological processes for the Day River Basin using remote sensing data on land use, rainfall, actual evapotranspiration, and Leaf Area Index (LAI). Knowledge of soil and vegetation parameters is a proper basis for quantification of the natural and anthropogenic eco-hydrological processes at un-gauged basins. This is the novelty of the paper as it demonstrated a methodology to assess terrestrial eco-hydrological processes and the translation into ecosystem services that are benefiting human beings in the Day River Basin, such as total runoff, natural livestock feed production, fuelwood from natural forests, dry season flow, groundwater recharge, root zone storage for carrying over water from wet to dry season, sustaining rainfall, peak flow attenuation, carbon sequestration, microclimate cooling, and meeting environmental flow requirements. It is shown that eleven selected HESS from [12] can be computed from a SWAT model that is calibrated with remote sensing data and that this methodology could become a routine effort to support the preparation of longer-term water resource plans.

2. Materials

2.1. Study Area

The Day Basin, located in Northern Vietnam, is a sub-basin within the transboundary Red River system (Figure 1). The area is approximately 6300 km^{2,} and the rainfall is 1700 mm/y. The Day Basin comprises several river tributaries, among which the largest is the Day River, with a total length of approximately 250 km. The Day Basin has a high biodiversity with abundant flora and fauna in the forested hills, freshwater aquatics, and wetlands, although agricultural land use is dominant. Topographical elevation ranges from low-lying delta (~0 m amsl) to mountainous areas (~1100 m amsl). The major land cover in the Day Basin is agricultural land (64%), followed by forested land (24%) and mixed mosaic (12%). An amount of 3100 km^2 (76%) of agricultural land is irrigated. The land use–land cover map contains 14 classes, and they form an essential input for the evaluation of HESS.

The Day Basin hosts the country's capital of Hanoi, an essential economic hub with an impact on prosperity in the basin. The climate in the Day Basin has a monsoonal character. The wet season elapses from May to October, and the dry season from November to April. The contribution of precipitation is mainly from rainfall, as there is no snowfall in the Day Basin. Precipitation can reach up to 450 mm per month in some parts of the basin. Over against that, precipitation can be as low as a few mm during January and February.

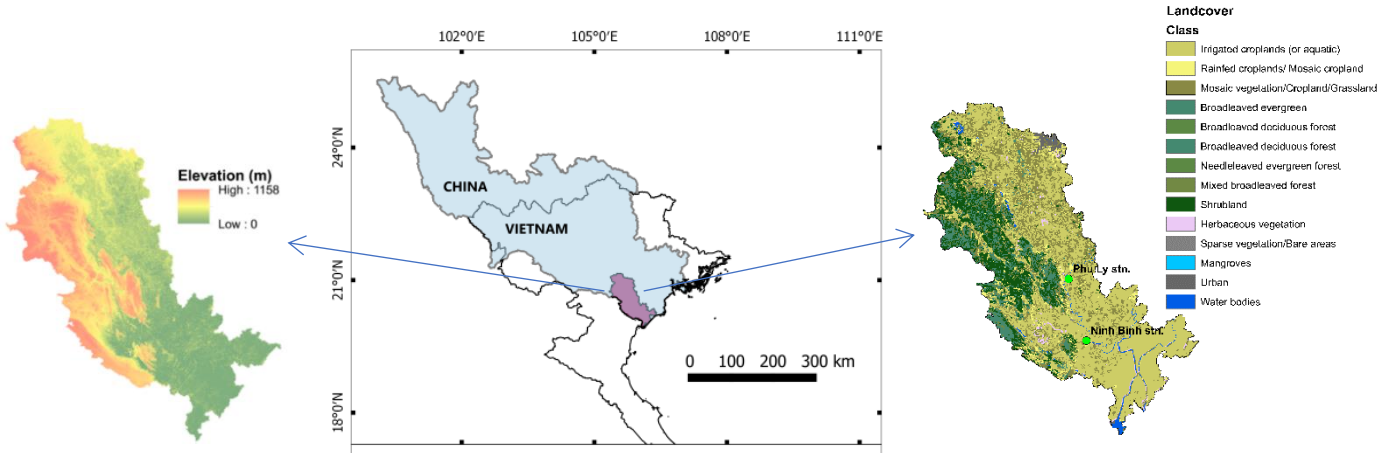

(**a**) (**b**) (**c**)

Figure 1. (**a**) Digital Elevation Map of the basin; (**b**) Geographical location of Day Basin as part of the Red River Delta in Northern Vietnam and (**c**) Land cover map of Day Basin.

2.2. SWAT Model Input Data

The input data into SWAT is based on spatial input data layers, wherever possible. Following [46], precipitation (P) in SWAT is derived from the Climate Hazards Group Infrared Precipitation with Stations (CHIRPS) data. Other climatic forcing data, e.g., radiation, wind speed, wind direction, daily minimum and maximum temperature, etc., was derived from the Global Land Data Assimilation System (GLDAS). The actual evapotranspiration (ET) used for SWAT was an ensemble product of 4 different datasets, namely CMRSET, SSEBop, MOD16, and SEBS [47,48]. The Leaf Area Index data is taken from the routine MODIS products. Observed streamflow data from 2003–2013 has been used in this study to calibrate the soil water balance. Daily measurements were taken from the discharge stations of Ninh Binh and Phu Ly (Figure 1c). Ha et al., 2022 [12] composed a list of remote-sensing datasets and derived parameters that can be used to quantify HESS. For instance, biomass production-related parameters, e.g., land surface temperature, Net Primary Production (NPP), can be derived from Landsat, MODIS Terra/Aqua, or Sentinel missions. Other parameters, such as precipitation, were reviewed and assessed the accuracy using criteria such as percent bias (PBIAS), Nash-Sutcliffe Error (NSE), and mean absolute error (MAE). Ha et al. [46] concluded that precipitation product such as CHIRPS shows a good corre-

lation with field measurements as compared with other products such as TRMM. Table 1 summarizes the input data used to execute the SWAT model for the Day Basin.

Table 1. Description of open access spatial data and their resolutions used in the study.

Data	Description	Resolution	Source
DEM	SRTM 30 m global DEM	30 m	Farr, T.G. et al. (2007) [49]
Soil	Coupled FAO and ISRIC soil maps	1 km	Ha et al. (2018) [46]
Land cover	GlobCover global land cover map	300 m	Arino et al., 2008 [50]
Precipitation	Daily precipitation from CHIRPS	5 km	Ha et al. (2018) [46]
Meteorology	GLDAS	25 km	NASA Goddard Earth Sciences Data and Information Services Center (GES DISC) [51]
ET	Ensemble ET	500 m	Ha et al. (2018) [46]
LAI	MODIS LAI	250 m	MOD15-LAI data (NASA EOSDIS Land Processes DAAC, USGS Earth Resources Observation and Science (EROS) Center, Sioux Falls, South Dakota, U.S.) [52]

2.3. Remote Sensing and SWAT Modeling Approach

The SWAT computes vertical and horizontal water flows and fluxes for each Hydrological Response Unit (HRU). One HRU has similar soil and vegetation properties but can be geographically dispersed so that they can be located in different parts of the sub-basin. There is no spatial variability present within HRU. The unsaturated zone is a combination of the root zone, a transition zone, and the capillary fringe that together form the vadose zone. The saturated zone is composed of a shallow and deep aquifer (see Figure 2). Lateral flow or interflow occurs from the unsaturated zone. Base flow occurs from the shallow aquifer.

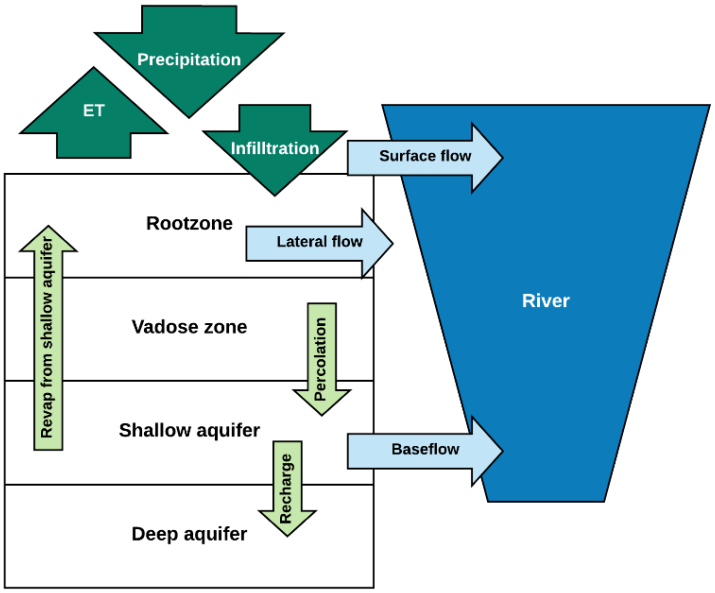

Figure 2. Schematization of vertical and horizontal water fluxes in an HRU in SWAT.

The calibration of SWAT requires various soil and vegetation parameters to be optimized to ensure a rigorous representation of surface runoff, recharge, base flow, soil moisture storage, net primary production, etc. SWAT-CUP appeared to be a very useful auto-calibration and uncertainty analysis tool for SWAT. A total number of 15 SWAT model parameters that are closely linked to the evolution of ET and LAI have been optimized. The numerical range of these model parameters affecting ET and LAI was derived from the SWAT user's manual [53]. The long list is based on the fact that one parameter might control more than one physical process, e.g., soil water-holding capacity affects the generation of overland flow but also determines water uptake by roots and percolation losses to the deeper underground. Earlier works with SWAT and sensitivity assessment recommended different parameters needed for the calibration [54–56].

SWAT parameters ESCO, EPCO, REVAPMN, SOL_K, SOL_AWC, and SOL_BD mainly affect ET. ESCO is the soil evaporation compensation factor that reflects the effect of capillary rise, crusting, and cracks. EPCO is the plant uptake compensation factor that controls the amount of water uptake by roots and the drought sensitivity of vegetation. REVAPMN is the threshold depth of water (in mm) in the shallow water aquifer for 'revap' or capillary rise from the deep aquifer to occur. SOL_K, or saturated hydraulic conductivity, relates soil water flow rate or flux density (in mm/h) to hydraulic conductivity. SOL_AWC is the plant's available water (in mm H20/mm soil). SOL_BD, or the moist bulk density (in mg/m^3 or g/cm^3), is the ratio of the mass of solid particles to the total volume of the soil. The baseflow recession constant ALPHA_BF and SCS runoff curve number (CN2) influence the actual water storage in the unsaturated zone and root zone.

Apart from soil evaporation parameters, the calibration of a distributed SWAT model involved modeling plant physiological characteristics to ensure a well-represented river basin's terrestrial eco-hydrological processes such as runoff, evapotranspiration, and plant and crop growth. With regard to plant physiology, six parameters are identified that influence the leaf area index development, see [57], which are very important for the quantification of the photosynthesis and the subsequent carbon assimilation process: BLAI, ALAI_MIN, LAIMX1, LAIMX2, DLAI, FRGRW1, and FRGRE2. BLAI is the maximum potential leaf area index (m^2/m^2). ALAI_MIN is the minimum leaf area index for the plant during the dormant period (m^2/m^2). LAIMX1 and LAIMX2 are the fractions of the maximum leaf area index corresponding to the 1st and 2nd points, respectively, on the optimal lead area development curve. FRGRW1 and FRGRW2 are fractions of the plant growing season or fractions of total potential heat units corresponding to the 1st and 2nd point, respectively, on the optimal leaf area development curve. DLAI is the fraction of the growing season when the leaf area begins to decline. These parameters are crucial to obtain plant physiological characteristics as described in Equation (A7). More details on the calibration process are described and demonstrated in [46]. SWAT-CUP solves all these model parameters for every Hydrological Response Unit. An HRU exists of various non-contiguous polygons with commonalities in soil type, slope, and land use. There are approximately 7000 HRUs in the Day Basin. The water balance, and hence all HESS values presented later, are computed for each HRU.

The results are displayed for HRU (e.g., distributed representation) for the HESS on total runoff, natural livestock feed production, fuelwood from natural forest, groundwater recharge, root zone storage, sustaining rainfall, carbon sequestration, and microclimate cooling. HESS, such as dry season flow (baseflow), peak flow attenuation, and meeting environmental flow requirements, are shown for river sections (i.e., directional polygonal representation).

3. SWAT-Modeling Framework for HESS

There are different analytical solutions to quantify the remaining HESS indicators. Ha et al. [12] presented a framework of 17 HESS that could be measured to support river basin plans and environmental monitoring. Within this framework, HESS is categorized into Provisioning services (HESS1: Total runoff, HESS2: Inland capture fishery, HESS3: Natural livestock feed production, HESS4: Fuelwood from natural forest), Regulating

services (HESS5: Dry season flow ("baseflow"), HESS6: Total groundwater recharge, HESS7: Surface water storage, HESS8: Root zone water storage, HESS9: Sustaining rainfall, HESS10: Peak flow attenuation, HESS11: Carbon sequestration, HESS12: Reduce Greenhouse Gas Emissions, HESS13: Micro-climate cooling, HESS14: Natural reduction of eutrophication in water, HESS15: Reduction of soil erosion), Supporting services (HESS16: Meeting environmental flow requirements), Cultural services (HESS17: Leisure). This paper aims to present the spatial determination of eleven selected HESS, i.e., HESS1, HESS3, HESS4, HESS5, HESS6, HESS8, HESS9, HESS10, HESS11, HESS13, and HESS16, which were computed from a SWAT model combined with remote sensing data.

3.1. Water-Related Provisioning Services

3.1.1. Total Runoff (HESS1)

Total runoff is the source of all blue water resources (streams, rivers, lakes, lagoons, aquifers), and it describes the longer-term renewable water resources provided to mankind and is originally based on rainfall and snowfall somewhere in the catchment. Some of this water is withdrawn by natural ecosystems, including groundwater ecosystems, and is thus not available for withdrawal. Total runoff is the combination of surface runoff, lateral flow, and base flow:

$$\boldsymbol{Q_{total} = Q_{surf} + Q_{lat} + Q_{bf}} \quad (1)$$

where Q_{total} p(m^3/ha) represents the total runoff, Q_{surf} (m^3/ha) is the horizontal fast overland flow, Q_{lat} (m^3/ha) is the horizontal interflow that occurs from lateral drainage processes in undulating terrain, and Q_{bf} (m^3/ha) represents the horizontal seepage that drains saturated soil towards rivers. The determination of these component flows was extensively discussed in the literature [58]. Appendix A explains a step-wise calculation of Q_{surf}, $Q_{lat,}$ and Q_{bf} that can be used to determine HESS1. For the sake of science and progressive insights into the HESS mechanisms, runoff is computed with current and historic land use; hence historic land use is taken as the reference. Landscape modifications such as the building of reservoirs and urban areas have affected the natural rainfall–runoff process. Pristine land cover with more forests and pastures will increase the total runoff generated in the Day Basin.

3.1.2. Natural Livestock Feed Production (HESS3)

The livestock in the Day Basin consists of buffalo, cows, and goats. Feed production for livestock comprises approximately 48% of grasses [59]. The other part has to come from feed crops or remnants of food crops. Three land cover classes in the Day Basin are found potentially suitable for grazing: mosaic crop, cropland, and mosaic vegetation crop. The cropland is, however, not natural for livestock, and mosaic crops are planted for food production, so only the land-cover class of mosaic vegetation crop is considered in the following analysis. The mosaic vegetation crop in the Day Basin comprises 2746 km^2. The plant physiological equation demonstrating actual plant growth in SWAT is:

$$\boldsymbol{\Delta Bio = \Delta Bio_{max}.\{1 - max(w_{strs}, t_{strs}, n_{strs}, p_{strs})\}} \quad (2)$$

where ΔBio_{max} is the potential increase in total plant biomass on a given day (g/m^2/d) derived from the light use efficiency of the plant (LUE) and the amount of Absorbed Photosynthetically Active Radiation (APAR) as described in Appendix A. $w_{strs}, t_{strs}, n_{strs}, p_{strs}$ describe the stress scalars that represent water, temperature, nitrogen, and phosphorous. Contrary to other crop growth models, SWAT considers only the maximum stress indicator out of these four. The water stress factor is governed by the actual and potential transpiration fluxes. The annual biomass production is a simple accumulation of ΔBio for the entire cycle and reflects the total dry matter production of fresh leaves, stems, roots, flowers, grains, tubers, and bulbs. The first distribution of the crop organs is between above-ground and below-ground accumulated biomass. This is classically expressed by means of the shoot/root ratio. Further to that, not all above-ground biomass production is taken for

livestock feed. The fraction of above-ground biomass production was taken as 65 percent of the total biomass production, and 40 percent of this amount is taken as natural livestock.

3.1.3. Fuelwood from Natural Forest (HESS4)

Forests are important sources of fuelwood [60]. The broadleaved, deciduous, and evergreen land-cover classes are considered to be representative of natural forests. The ratio of the above and below-ground biomass production for natural landscapes has been measured for several biomes. [61] estimated the below-ground biomass to be 0.25–0.30 of the above-ground biomass, using plant growth simulation models. The fraction of above-ground biomass production usable as firewood is taken as five percent (e.g., dead wood, debris). The simulation of the increase in biomass is demonstrated in Equations (A6) and (A7) in the Appendix A.

The SWAT computes the net carbon assimilation for natural forests in a similar biophysical manner as was done for crops and mosaic vegetation. Woody plants are–however–characterized by secondary growth and continuous conversion of structural tissue into non-living, therefore non-respiring biomass. To simulate the smaller amount of biomass accumulation seen in seedlings/saplings, tree growth within a single year is limited to a fixed amount determined by the age of the tree relative to the number of years for the tree species to reach full development. Parameters in the plant growth database define the total number of years for trees to reach full development as well as the biomass of a fully-developed tree. Once the total growth in biomass in a year, bio reaches the annual limit; no more growth occurs until the next year when a new annual limit is calculated.

3.2. Water-Related Regulating Services

3.2.1. Dry Season Flow (HESS5)

Base flow is highly desirable to meet the water demands from domestic and industrial requirements during the dry season, besides keeping a minimum environmental flow for fish stocks. Water percolating past the bottom of the root zone is partitioned into two fractions: a shallow and deep aquifer. Water stored in the shallow aquifer may replenish moisture in the soil profile in very dry conditions by means of capillary rise or be directly removed by deep rooting plants (REVAP). Groundwater-dependent ecosystems, for instance, tap directly into these unconfined aquifers. The remaining water stored in the shallow aquifer flows to the river as a classical lateral drainage flow. Water from the deep aquifer flows out of the watershed and does not contribute to dry season river flow.

The dry season flow in Day Basin relates to the dry period between November-April (6 months). For all the major streams of Day Basin, the average dry season flow (m^3/s) is computed as:

$$\boldsymbol{Q_{bf,i} = Q_{bf,i-1}.exp\left(-\alpha_{gw,shi}.\Delta t\right) + w_{rchrg,sh,i}.\left[1 - exp\left(-\alpha_{gw,sh}.\Delta t\right)\right]} \quad (3)$$

where $Q_{bf,i}$ is the baseflow from a shallow aquifer on day i (mm), α_{gw} is the baseflow recession constant, Δt is the time step (1 day), $w_{rchrg,sh,i}$ is the amount of recharge entering the shallow aquifer (mm).

3.2.2. Total Groundwater Recharge (HESS6)

Groundwater recharge describes the replenishment of aquifers. Aquifers should be considered as savings accounts for periods of water storage, and this describes the cap of groundwater withdrawals. The total recharge to the aquifer on a given day is calculated as an exponential decay weighting function based on hydrological conditions. It is neither related to land use nor the source of water. Hence the total recharge includes water from floods, irrigations, leaking rivers, and more. The delay function accommodates situations where the recharge from the soil zone to the aquifer is not instantaneous:

$$w_{rchrg,i} = \left[1 - exp\left(-\frac{1}{\delta_{gw}}\right)\right].w_{perc} + exp\left(-\frac{1}{\delta_{gw}}\right).w_{rchrg,i-1} \quad (4)$$

where $w_{rchrg,i}$ is the amount of recharge entering the aquifers on day i (mm/d), δ_{gw} is the delay time or drainage time of the overlying geologic formations (day), w_{perc} is the total amount of water exiting the bottom of the soil profile on day i (mm) (calculated as in Appendix A), and $w_{rchrg,i-1}$ is the amount of recharge entering the aquifers on day $i - 1$ (mm). Without the delay time δ_{gw}, recharge equals seepage. Percolation occurs if the drainable volume of water in the soil layer on a given day exceeds field capacity. If a given HRU has a seasonably high water table, then percolation is not allowed.

3.2.3. Root Zone Storage (HESS8)

The root zone depth is the depth within the soil profile that commodity crop (cc) roots can effectively extract water and nutrients for growth. The presence of roots in the soil matrix develops certain matric potentials that increase the retentive forces to hold water for a certain period. For many vegetation types, the root zone depth is constant with time, and the deeper the roots, the more water can be retained. For non-perennial vegetation, SWAT computes root development on the basis of heat units. The root depth and root density are a fraction of the total biomass production and the shoot/root ratio. In addition to that, soil moisture is also stored in the vadose zone between the lower part of the root zone and the depth of the unconfined groundwater table. Reference work [62] showed a simplified method to assess changes in soil moisture in the entire vadose zone based on the average soil moisture content in the root zone and an equilibrium soil water potential distribution below up to the phreatic level where retention is absent. In SWAT, the change in soil moisture between the end of the rainy season and the start of the next rainy season is used as an indicator for storage change:

$$\Delta S_{\theta} = \int \theta(z).dz(t) - \int \theta(z).dz(t+1) \quad (5)$$

where ΔS_{θ} is the storage change for the entire unsaturated soil profile, thus including the root zone and the vadose zone at t (end of rainy season) and $t + 1$ (end of the dry season), $\theta(z)$ is the moisture content at depth z at t (end of rainy season) and $t + 1$ (end of the dry season), and dz is the soil profile depth. For practical reasons, the total soil depth of 100 cm is considered for HESS8 because the underground is rocky at locations, although this could be improved with the inclusion of a root depth for each land-use land-cover class.

3.2.4. Sustaining Regional Rainfall (HESS9)

Usually, the evaporated water is considered to have been consumed and is no longer available for downstream water use. However, regional rainfall processes can also be triggered by local evaporation processes. Convectional rainfall occurs, for instance, when the warm air deflected from a landform rises and is full of water vapor originating from land surface evaporation. Convectional rainfall is more severe in tropical areas where climates are warmer. Reference work [63] demonstrated that the tropical forests in Africa generate their own rainfall. Hence, it seems that not all evaporated water is truly consumed, and it is very interesting to understand which part of the evaporated water contributes to sustaining regional rainfall within the same basin.

Reference work [64] showed that globally, nearly 20% of the total yearly precipitation on land originates from vegetation evaporation-regulated moisture recycling, with large spatial variability. For the Day Basin, 40% of the annual rainfall originates from upwind, continental-scale land evaporation [65]. A lower evaporation recycling ratio is expected when the evaporative surface has to be located inside the geographic boundaries of the Day

Basin. An unpublished study [66], using a simple atmospheric moisture accounting scheme, showed that less than 10% of rainfall in the Day Basin is recycled from evapotranspiration.

$$\boldsymbol{P_{sus} = P - P_{adv} = \alpha ET} \quad (6)$$

where P_{sus} is the sustained rainfall due to local evaporation processes (mm/y), P_{adv} is the rainfall that originates from external sources (mm/y), α is the evaporation recycling ratio, P is precipitation rate (mm/y), and ET is the evapotranspiration rate (mm/y). A pragmatic value of α = 7.5% has been applied for this Day Basin study.

3.2.5. Peak Flow Attenuation (HESS10)

The purpose of HESS 10 is to show to which extent the presence of vegetation reduces peak flow. A more comprehensive modeling should also include the presence of (wet) land located nether rivers that can be used for inundation. Consumptive use of vegetation has several by-products, and peak flow attenuation due to decreased surface runoff is one of them. SWAT automatically generates main categories of reaches on the basis of the Digital Elevation Model. Stream flow in every reach of the catchment was computed first on the basis of 100% bare soil conditions. A monthly flood with a return period of 1 out of 10 years was used as a baseline in every HRU above which flood hazard prevails. For practical reasons, longer periods of consideration were not feasible due to the absence of high-quality remote sensing data. Monthly flows between June and October were considered for every reach of a major stream.

During a second SWAT model run, actual land use and LAI status were used instead of bare soil. Due to a different Curve Number value and antecedent soil moisture, the retention will increase, and surface runoff Q_{surf} will decrease. A reduction of Q_{surf} will undoubtedly lower the number of events with flow exceeding the threshold value. The calculation of the retention parameter is provided in Appendix A. The peak flow attenuation (%) was calculated as the relative difference of the number of peak flows; the results confirm that the number of peak flow events decreases due to the presence of vegetation.

3.2.6. Carbon Sequestration (HESS11)

Net carbon assimilation is responsible for the growth of plant organs. The different organs have various life cycles. Crop residues and litter are generally conceived as short-term carbon storage; carbon from these organs is often released again into the atmosphere during the same year. Soil organic carbon and harvested stems have a significantly longer time scale. The sequestration of carbon for HESS11 relates to wood from trees and soil organic carbon.

Carbon sequestration is a fraction of biomass production (CH_2O). One unit of sequestrated carbon C is equivalent to 12/30 (calculated from the molecular weight) or 0.4 unit of biomass if biomass consists entirely of carbon hydrates. Because of other substances present, it is more convenient to use a factor of 0.45. IPCC 2006 Guidelines for National Greenhouse Gas Inventories Volume 4 Agriculture, Forestry, and Other Land Use [67] also suggested a range between 0.43 and 0.55.

Further to C/biomass ratios, the shoot/root ratio is a critical element in describing organ distributions. [68] found that for most tree species in Sweden above-ground biomass is 65% of the total biomass production value, being equivalent to a shoot/root ratio of 1.85. Cereal crops have typical shoot/root ratios of 2.0 (barley), 4.0 (rice), to 5.0 (wheat). Root crops have much lower shoot/root ratios (0.25 to 0.5) because the harvestable product is essentially formed below ground. Carbon sequestration is not computed in SWAT but can be approximated using the partitioning factors. For trees and shrubs, the above-ground carbon stored per year can be approximated is:

$$C_{ag}=\frac{0.45.S_r}{(S_r+1)}\sum Bio \quad (7)$$

where Sr is the shoot/root ratio being 1.85 for trees, $\sum Bio$ is the increase in biomass. The above-ground C-sequestration is $0.29\sum Bio$.

The below-ground biomass is partitioned into root mortality and exudation, as well as soil organic matter from litter, dead wood, root mortality, and exudation. The humification coefficient for converting dry matter into soil organic matter is typically 0.35 [69]. If we, for simplicity, assume 35% of below-ground biomass to be sequestered, then it can be approximated mathematically as:

$$C_{bg}=0.35x0.45x\left\{1-\frac{S_r}{(S_r+1)}\right\}\sum Bio \quad (8)$$

Note that above-ground crop residues can also be considered as an input for soil organic carbon, but then this material must be plowed or disked in. Rice is a key crop in Day Basin, and a shoot/root ratio of 4.0 is taken, see [70]. The annual carbon storage for rice then becomes $0.02\sum Bio$. Hence, the sequestrated carbon is 2% and 34% of the total crop biomass production for crops and woody vegetation (shrubs and trees), respectively.

3.2.7. Microclimate Cooling (HESS13)

Photosynthesis creates evaporative cooling over green and biologically active vegetation. The transpiration process requires a considerable amount of energy (1 mm/d is equivalent to approximately 2.5 MJ/d). This energy is not available for sensible heat flux H, so H over an evaporative surface is usually small. Reference work [71] reviewed H flux measurements over water-evaporating surfaces and concluded that H is negligibly small. Climatic cooling at the local scale not only reduces the vegetation water requirements but also suppresses the land surface and air temperature in, for instance, urban heat islands [72]. The change in sensible heat flux can be converted into a change in air temperature. H is not computed explicitly in SWAT but was determined afterward by subtracting net radiation Rn and latent heat flux LE (W/m^2) (as described in Appendix A).

The conceptual model of HESS13 is that it lowers the difference in temperature (ΔT) as compared to ΔT under conditions of bare soil (with lower ET fluxes). Presumably, the change in the surface roughness's effect on heat transfer is negligible, and R_n stays constant in the two cases; the microclimate cooling (degree Celsius) was calculated as:

$$\Delta T_{cooling}=\Delta T_{soil}-\Delta T_{veg}=\frac{r_{ah}}{\rho_a.C_p}\left(H_{soil}-H_{veg}\right)=\frac{r_{ah}}{\rho_a.C_p}\left(LE_{veg}-LE_{soil}\right) \quad (9)$$

With ΔT_{soil} being the difference in temperature with bare soil as a reference land cover, ΔT_{veg} being the difference in temperature with vegetation cover (current land cover), H and LE is sensible and latent heat flux (W/m^2), ρ_a being the density of moist air, C_p is the specific heat at constant pressure for air (1004 J/kg·K), and r_{ah} is aerodynamic resistance to heat transfer that we fixed at 70 s/m following [73].

3.3. Water-Related Habitat/Supporting Services

While SWAT has pesticide fate components, cycles for nutrients and bacteria, and route metals through reaches [57], all these functions require proper parameter estimations that could not be accomplished. For this sake, soil formation, erosion, and nutrient simulations are excluded from the analysis in the Day River, and the emphasis will be more on environmental flow requirements.

Meeting Environmental Flow Requirements (HESS16)

The vitality and biodiversity of riverine and wetland ecosystems require a certain flow regime such as (i) magnitude, (ii) frequency, (iii) timing, (iv) duration, and (v) the rate of

change of inter and intra-annual events. According to the Brisbane Declaration of 2018, these aquatic ecosystems include rivers, streams, springs, riparian, floodplain, and other wetlands, lakes, coastal waterbodies, including lagoons and estuaries, and groundwater-dependent ecosystems. This flow regime results in a certain minimum low flow and consumes water through the ET from open water bodies and wetland vegetation [74].

Reference work [75] assessed the mean environmental flow requirements for 128 major basins and drainage regions worldwide using measured and simulated hydrographs. Five different environmental classes were considered. While his work has a good solid basis, in the end, they came up with very generic guidelines. A fraction of 0.28 of the mean annual flow is suggested as the environmental flow for the Mekong Basin region. For the Red River Basin, [76] suggests a fraction of 0.29. While we recognize that water demands associated with the maintenance of the health of riverine ecosystems in the Day River can be improved, we just use the 0.29 fraction as suggested. HESS16 is defined as the degree of satisfaction to meet the environmental flow requirement ($Eflow_{sat}$) on a yearly basis:

$$\boldsymbol{Eflow_{sat}}\textbf{=100\% } \boldsymbol{if} \ \frac{\boldsymbol{Q_{lowflow}}}{\boldsymbol{Q_{yr-longterm}}} \geq \textbf{0.29} \tag{10}$$

$$\boldsymbol{Eflow_{sat}}\textbf{=}\frac{\boldsymbol{Q_{lowflow}}}{\textbf{0.29}\boldsymbol{Q_{yr-longterm}}}\textbf{.100\% } \boldsymbol{if} \ \frac{\boldsymbol{Q_{lowflow}}}{\boldsymbol{Q_{yr-longterm}}} \textbf{<0.29} \tag{11}$$

$Q_{lowflow}$ is the total flow during six dry months (November–April). $Q_{yr\text{-}longterm}$ is the average annual flow.

4. Spatial Mapping of HESS for Day Basin

The HESS values of the Day River were simulated for the period 2000 to 2013 using three years of initialization (2000–2002) as a warming-up period. The period 2000–2013 was chosen as the study period under the CGIAR WLE's funded project *"Inclusive development paths for healthy Red River landscapes based on ecosystem services."* Although the time step of the model is daily, most outputs are presented as an annual result or longer time scale. The spatial discretization is by HRU.

4.1. Water-Related Provisioning Services

Figure 3a shows the spatial distribution of HESS1 on generated total runoff in the basin. The areas with high capacities for total runoff are in the mountainous and highly dense forest cover on sloping terrain (15,000 m^3/ha and more). The urban area of the basin shows a higher total runoff due to poor infiltration and overall large CN numbers. The Day Basin averaged total runoff is 7482 m^3/ha/y.

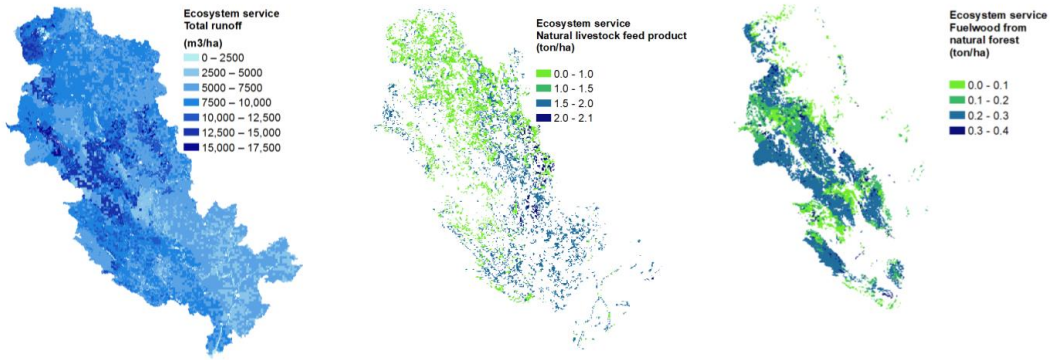

(**a**) (**b**) (**c**)

Figure 3. Provisioning service for Day Basin during 2003–2013 for (**a**) HESS1: Total runoff (m^3/ha/y); (**b**) HESS3: Natural livestock feed production (ton/ha/y); (**c**) HESS4: Fuelwood from the forest (ton/ha/y).

Figure 3b shows the mean annual distribution of HESS3 on natural livestock feed production (ton/ha/y) in the Day Basin during the study period. The results relate to mosaic crop areas only because other land use classes do not provide natural feed for livestock. The western part of the basin experiences areas without feed production. The Day Basin average feed production for livestock (including land surfaces with zero values) is 0.3 tons/ha/y.

The HESS4 on fuelwood production (ton/ha/y) taken from the natural forest of the Day Basin is presented in Figure 3c. Since this service originated only from natural forest land cover, the results reflect the dry matter production of forests. The areas in the mountainous part of the basin in the west experienced a higher production (0.3–0.4 ton/ha) as compared with other areas. The average value for the Day Basin (including land surfaces with zero values) is 0.013 tons/ha/y.

4.2. Water-Related Regulating Services

HESS5 on dry season flow (m^3/s) in Figure 4a is a very important natural ecosystem service that provides a source of water for local communities during the long dry season, apart from being key to meeting the water demands of fluvial ecosystems. The discharge is low at the origin of streams (0–10 m^3/s), and this swells to more than 100 m^3/s in the tail end of the basin. This flow is averaged for the six dry months running from November to April. Communities at the downstream end thus have more access to dry season water resources. The average flow for these major tributaries is 113 m^3/s, while the basin average, including upstream and downstream areas, is 12 m^3/s.

HESS6 on total groundwater recharge ($m^3/ha/y$) displayed in Figure 4b shows higher HESS contributions in the forests of the northwest of the Day Basin (6000–7200 $m^3/ha/y$). This is mainly related to the higher rainfall regimes that are common for forested mountains. The forests have a positive impact on enhanced infiltration and reduced surface runoff (unless grown on sloping terrain). This total recharge presents vast quantities of groundwater that will be exploited for both natural and anthropogenic usages. The average total groundwater recharge is 3820 $m^3/ha/y$.

The root zone storage (i.e., HESS8) is shown in Figure 4c. HRUs that contain open water bodies are excluded from the analysis to comply with root systems only. The results show a nice complementary relationship between HESS6 and HESS8; Areas with high HESS8 in the delta will have a low HESS6 and vice versa. Clearly, every agroecosystem in a complex river basin has its own share of the overall HESS performance. The average root zone storage for Day Basin is 1493 $m^3/ha/y$.

The delta contributes more to sustaining rainfall, i.e., HESS9 (Figure 4d), provided that the wind direction is inland in the direction of the hills. Moist air advection into the air mass over the Gulf of Tonkin will not sustain rainfall in the Day Basin. A similar conclusion was drawn by [77], who demonstrated that most of the rainfall in the Himalayas originates from irrigated wheat-rice crop rotations on the Indo-Gangetic plain. The average sustainable rainfall is 701 $m^3/ha/y$. Rice fields are thus obviously efficient contributors for generating rainfall in the upstream mountains that enhance recharge and dry season flow. It is an important finding that the consumptive use of rice is providing HESS in addition to provisioning food.

The attenuation of peak flow (i.e., HESS10) mainly follows the partitioning between infiltration and runoff by means of overland flow (Figure 4f). First, the SWAT model was executed with bare soil conditions to define the hydrograph statistics under reference conditions with an emphasis on daily peak flows. The reduction of these peak flow events was determined after running SWAT again with current land use practices. It is witnessed that natural landscapes such as forests and wetlands provide a wealth of regulating ecosystem services in detaining excess rainfall and, therefore, delaying peak flows. The average reduction of peak flow varies between 5 to 10%. An upstream-to-downstream accumulation is visible in Figure 4f; the lower part of the Day Basin is getting less susceptible to peak flows (15 to 20% reduction of natural peak flows). The role of forests in reducing peak flow has also been marked by others [78]. The average peak flow attenuation due to the current land use is 5.1%.

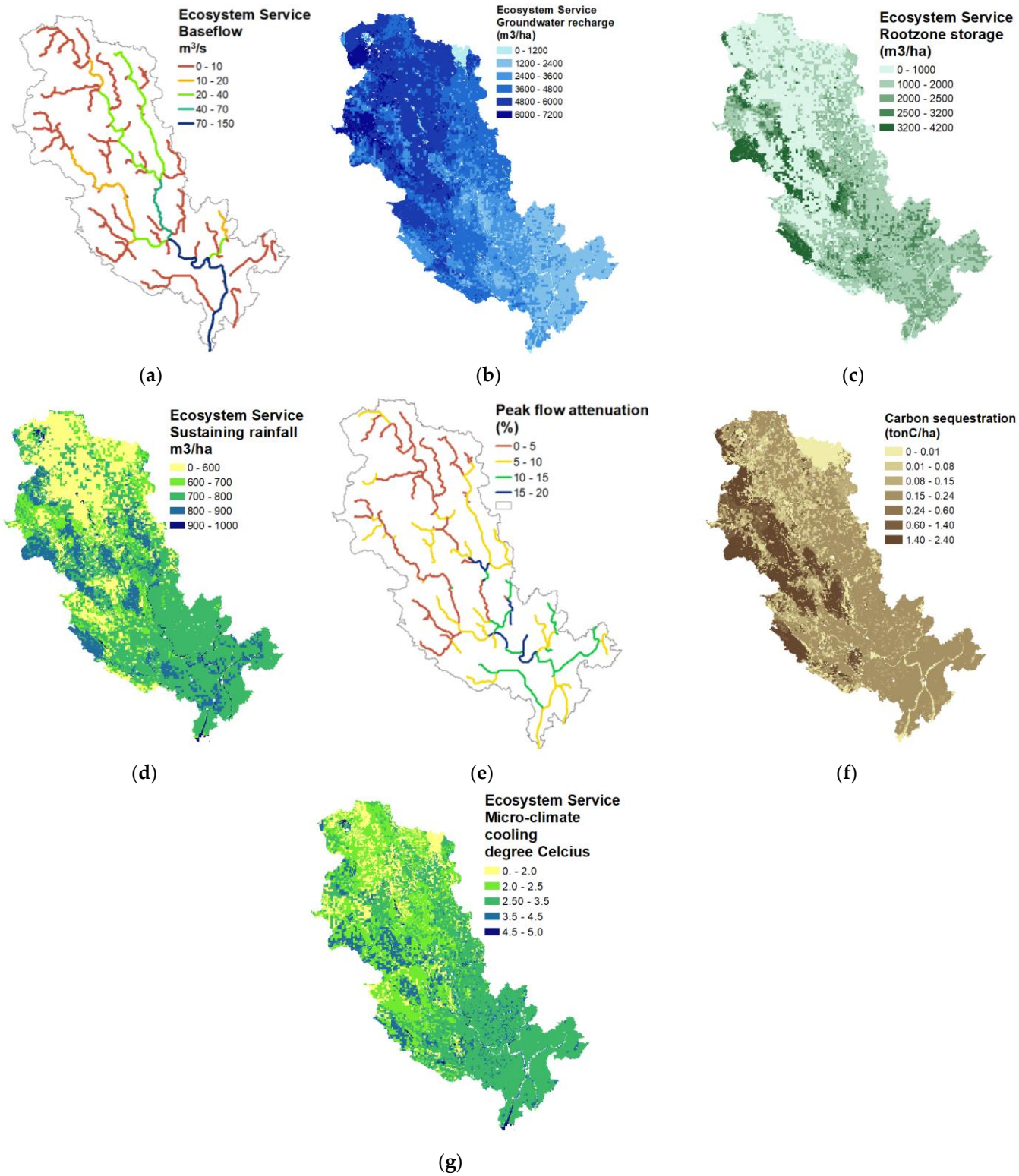

Figure 4. Regulating services for Day Basin with average value during 2003–2013 for (**a**) HESS5: Dry season flow or baseflow (m^3/ha); (**b**) HESS6: Groundwater recharge (m^3/ha); (**c**) HESS8: Root zone storage (m^3/ha); (**d**) HESS9: Sustaining rainfall (m^3/ha); (**e**) HESS10: Peak flow attenuation (%); (**f**) HESS11: Carbon sequestration (ton C/ha); (**g**) HESS13: Microclimate cooling (degree Celsius).

Atmospheric carbon sequestration in the Day Basin (HESS11) was quantified to vary between 0.01 to 2.4 tons/ha/y (Figure 4e). Natural forest in the western part of the basin sequesters up to 2.4 tons/ha/y. Urban areas and settlements have a much lower

sequestration process of approximately 0.01 to 0.1 ton ha/y. The Day Basin has an average atmospheric carbon sequestration of 0.22 tons/ha/y.

The role of a vegetation pack on reduced air temperatures (i.e., HESS13) is shown in Figure 4g. All values are positive, which implies that every landscape element creates a microclimate that can potentially offset temperature rises from global warming. The maximum cooling is 4.5 to 5 degrees Celsius, and this occurs in dense forests. The basin's average microclimate cooling is 2.7 degrees.

4.3. Water-Related Habitat/Supporting Services

The satisfaction of meeting environmental flow, i.e., HESS16 for a dry (2011) and wet year (2013), is illustrated in Figure 5. For every reach, the longer-term river flow was computed from SWAT, and the environmental flow was defined as 29% of the annual volume. The dry season flow in the six-month dry period in each year was compared against the environmental flow (e-flow), indicating whether it satisfied the threshold amount ($Eflow_{sat} = 1$) or not ($Eflow_{sat} < 1$). There is a clear-cut effect of wet and dry years on meeting the environmental flow (e-flow) requirement. While in the dry 2011, e-flow ranged from 20–80% in most upstream river stretches, this increased to nearly 80–100% in the wet year of 2013. In general terms, the lower delta in the Southeast better meets the environmental flows because the hydrograph responds to a larger catchment area where most variations in discharge are averaged out. The environmental flow satisfaction is 82% and 95% in a dry and wet rainfall year, respectively.

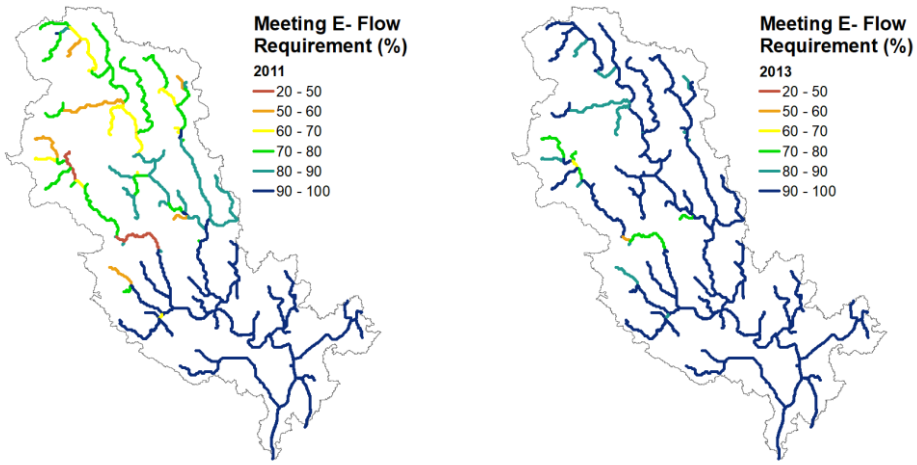

(**a**) (**b**)

Figure 5. Habitat services for Day Basin during 2003–2013 for meeting environmental flow for (**a**) dry year (2011) and (**b**) wet year (2013).

While Figures 3–5 show the spatial variabilities of the HRUs, Figure 6 describes the temporal variation of ecosystem services in the Day Basin during the period between 2003 and 2013. The standardized boxplots show the trade-offs between the HESS indicators and years. Total runoff (HESS1) and groundwater recharge (HESS6) show a tighter coupling to rainfall than biomass-related services such as feed production, fuelwood, and carbon sequestration. Adding a simple trend line through the average values and the quartiles will show the following insight: For HESS 1, 3, 4, and 6, the average values increase. For HESS 8 and 13, the average value decreases while the rest of the HESS, i.e., 5 and 11, show a more constant trend. Overall, the quartile values have more variation with time than the average values do. Hence, these mild extreme values are more vulnerable to external factors, such as rainfall and inflow from upstream rivers, than the average values.

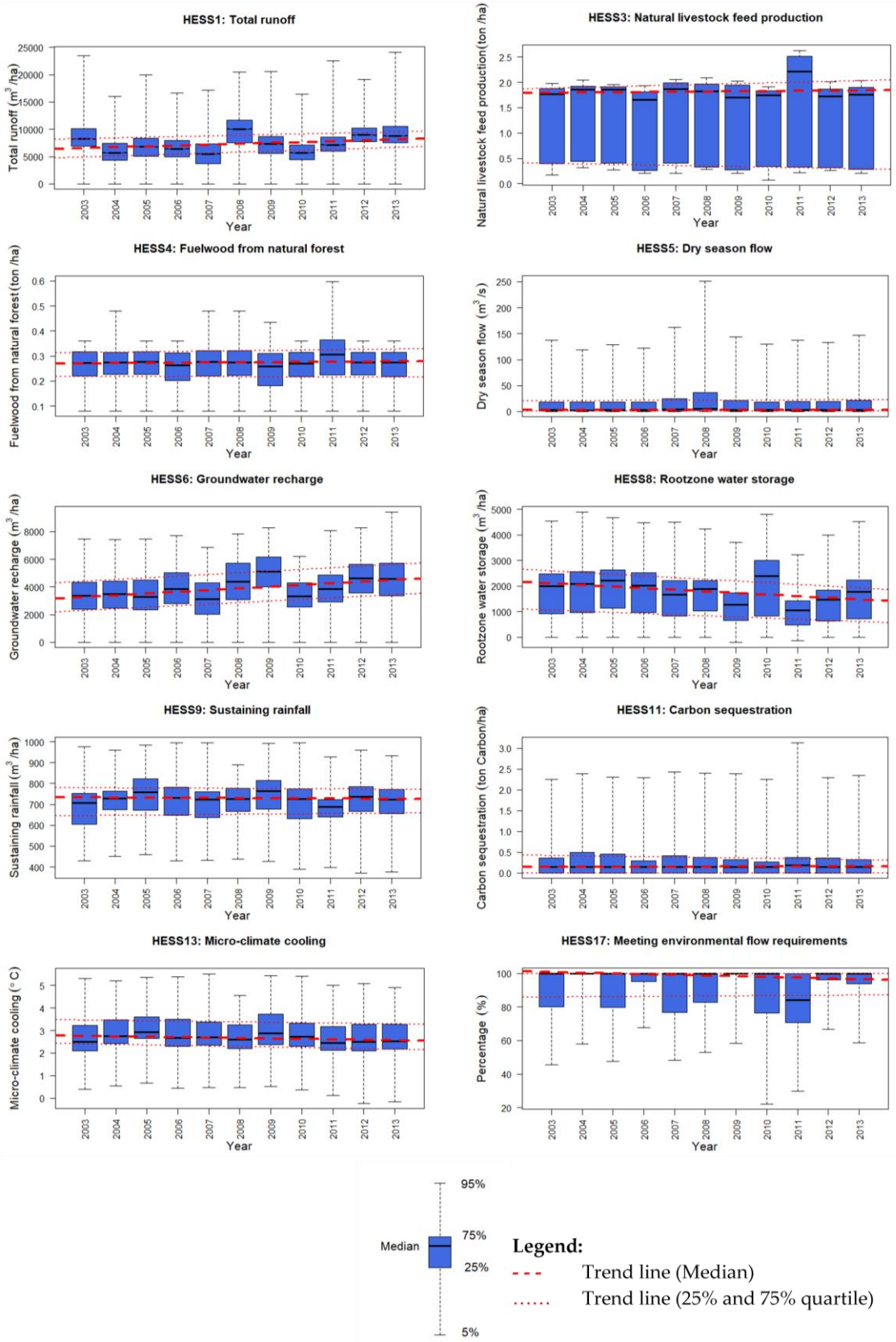

Figure 6. Boxplot values of ecosystem services for Day Basin from 2003–2013 and yearly average with median, quantile (5%, 95%), and quartile (25% and 75%). The dashed and dotted red lines show a trend line through the median, 25%, and 75% quartile, respectively.

For benchmarking between river basins mutually, and also for studying the impact of land use and water use planning scenarios on HESS, it is good to synthesize the major findings. Similar results were found with the Day sub-basin in the Red River by [79]. They investigated the impact of deforestation by thinning existing forests and projected climate change (by 2050, an increase of 1.5 °C and 6% rainfall). It was observed that the removal of forests increased sediment yield from the basin substantially and increased peak flows and corresponding flood hazards. In their study, seven out of 11 HESS values increased with climate change.

Focusing on a single HESS value thus provides an incomplete picture. Against this background, a synthesis table for the Day Basin was created (see Table 2).

Table 2. Synthesis table based on SWAT outputs as yearly average, gross value, and per capita.

Ecosystem Services	Average		Gross Value		Per Capita	
	Unit	Value	Unit *	Value	Unit	Value
HESS 1: Total runoff	m^3/ha	7482	MCM	4706	m^3/cap	392
HESS 3: Natural livestock feed production	ton/ha	0.3	MTonnes	0.2	ton/cap	0.01
HESS 4: Fuelwood from natural forest	ton/ha	0.013	MTonnes	0.008	ton/cap	0.001
HESS 5: Dry season flow ("baseflow")	m^3/s	12	MCM	372	m^3/cap	31
HESS 6: Groundwater recharge	m^3/ha	3820	MCM	2403	m^3/cap	200
HESS 8: Rootzone water storage	m^3/ha	1493	MCM	939	m^3/cap	78
HESS 9: Sustaining rainfall	m^3/ha	701	MCM	441	m^3/cap	37
HESS 10: Peak flow attenuation	%	5.1	-	-	-	-
HESS 11: Carbon sequestration	ton/ha	0.22	MTonnes	0.14	ton/cap	0.01
HESS 13: Micro-climate cooling	°C	2.7	-	-	-	-
HESS 17: Meeting environmental flow requirements	%	92	-	-	-	-

* MCM: million cubic meter; MTonnes: million tonnes.

Table 2 shows a synthesis of HESS values in terms of average, gross value, and per capita. The population of the Day River Basin in 2015 was 12 million. The average generated total runoff in the basin is 7482 m^3/ha, which contributes to a total gross value of 0.38 million m^3 (MCM) per year and a net per capita of 392 m^3. Other flow-related services, such as groundwater recharge, rootzone storage, and sustaining rainfall, achieved average values of 3820, 1493, and 701 m^3/ha, respectively. Gross groundwater recharge was 2403 MCM while per capita reached 200 m^3/cap. The average HESS8 on rootzone water storage and HESS9 sustaining rainfall was 1493 and 701 m^3/ha translating to a per capita of 78 and 37 m^3, respectively. Interestingly, microclimate cooling (HESS 13) indicated that the ecosystem of the Day Basin reduces the air temperature by 2.7 degrees Celsius (as compared to bare soil land cover). HESS 17 reached 92% during the period from 2003–2013, indicating that only during certain periods the requirement for environmental flow was not satisfied. Biomass-related HESS such as HESS 3 and 4 averaged at 0.3 and 0.013 ton/ha leading to gross values of 0.2 and 0.008 and per capita of 0.01 and 0.001 ton/ha, respectively. The sequestered carbon (HESS11) was 0.01 ton/cap/y.

Table 3 further describes the trendline established in Figure 6 for each HESS. The gradient and intercept of the trendline were derived, which display the observed trend of HESS. This information is crucial in indicating whether a HESS is maintained at a healthy state (upward trend) or degrading (downward trend). Based on this analysis, basin planners and water managers can justify their plans and policies in order to sustain or restore the functions of degrading HESS.

Table 3. Statistical performance of HESS trendline (gradient/slope) and implications into river basin plans.

Ecosystem Services	Gradient/Slope of HESS Trend	Interpretation of Trend and Impacts on HESS	Implication into River Basin Plans and Management
HESS 1: Total runoff	159	Increasing	Sustain basin management practices, implementation of IWRM
HESS 3: Natural livestock feed production	0.0044	Increasing	Sustain basin management practices
HESS 4: Fuelwood from natural forest	0.0008	Increasing	Sustain basin management practices
HESS 5: Dry season flow ("baseflow")	0.0215	Increasing	Improve application of IWRM and land-water management or Natural-based Solutions (NbS) practice
HESS 6: Groundwater recharge	122.3	Increasing	Apply Managed Aquifer Recharge (MAR) to better improve groundwater management
HESS 8: Rootzone water storage	−61.7	Decreasing	Improve basin management to facilitate soil-water interaction. Improve basin permeability through green building and permeable landscapes.
HESS 9: Sustaining rainfall	−0.68	Decreasing	Improve basin management, IWRM, and NbS to improve basin-scale soil moisture circulation
HESS 11: Carbon sequestration	0.0013	Increasing	Sustain current basin management practices, apply carbon credit system
HESS 13: Micro-climate cooling	−0.0191	Decreasing	Apply NbS, green building to reduce urban heat island effect. Improve IWRM and land-use planning
HESS 17: Meeting environmental flow requirements	−0.4249	Decreasing	Introduce IWRM in the basin, revise water plans, including sharing and allocation to prioritize e-flow contribution

5. Discussions

HESS have received public attention for a considerable time. The definition and quantification of HESS are rather complex and touch base with the core of multi-disciplinary environmental sciences. The assessment of important ecosystem processes with a minimum of anthropogenic influences requires complex algorithms. There are many good examples available using eco-hydrological models and remote sensing techniques [80,81]. Often these studies are, however, restricted to solving a few elements only, and they are applied in a local context where supporting input data are available. Ha et al. [12] established a HESS framework presenting 18 HESS that can be measured to support river basin plans and environmental monitoring, categorized into Provisioning services (four HESS such as total runoff, inland capture fishery, natural livestock feed production, fuelwood from natural forest), Regulating services (eleven HESS such as dry season flow, total groundwater recharge, surface water storage, root zone water storage, sustaining rainfall, peak flow attenuation, carbon sequestration, reduce greenhouse gas emissions, micro-climate cooling, natural reduction of eutrophication in water, natural reduction of (agro-) chemical in water, reduction of soil erosion), Supporting services (one HESS on meeting environmental flow requirements), Cultural services (one HESS on leisure). This paper touches base with 11 HESS indicators, which provides a more comprehensive picture than many other studies. Selected HESS, i.e., HESS1, HESS3, HESS4, HESS5, HESS6, HESS8, HESS9, HESS10, HESS11, HESS13, and HESS16 are deemed relevant to represent a broad spectrum of benefits to people in the Day Basin. It ranges from direct and primary benefits (e.g., food production, provision of runoff, fuelwood, etc.) to a larger bio-physical context such as micro-climate regulation, rootzone moisture, meeting e-flow requirement, etc.). These assessments provide a synthesized snapshot of marginal benefits to ecosystems and

humans resulting from basin management activities. The consideration of these eleven HESS in the Day Basin paves the way for human-centered and multi-criteria objectives for development and conservation.

The distribution and valuation of HESS highlight hydrological ecosystem services that benefit the basin and its population. While showing the Day Basin's abundant generation of the HESS in the total runoff, carbon sequestration, groundwater recharge, and rootzone water storage as compared to other global study sites [19,32,82], the high population significantly reduces per capita performance. Moreover, several HESS indicate a downward trend, e.g., rootzone water storage, microclimate cooling, and meeting e-flow requirements suggesting a thorough assessment and introduction of more sustainable approaches in land-use planning and basin management practices and land-use planning such as Integrated Water Resources Management (IWRM) or Natural-based Solutions (NbS) to enhance HESS values in the basin.

Potentially more HESS indicators could be included in the list, such as soil erosion, natural reduction of eutrophication and agrochemical in water, water storage in lakes, etc. The SWAT model has the capacity to include these extra HESS indicators as the model design is intrinsically meant to deal with describing the total environment of agroecosystems. Hence, the results presented in this paper are not exhaustive but should be regarded as a first step further in a direction with gradually more understanding and tools available to quantify HESS in a more routine manner.

Water productivity is a concept introduced by [83,84] to pinpoint the benefits and services of water consumption. Various studies computed the bio-physical and economic water productivities, e.g., [85], and others also included the job opportunities for water availability and water consumption. This paper shows that the concept of water productivity should be amended with a HESS component. Water consumption is not only good for food security, but it also generates rainfall, cools the atmosphere, sequesters carbon, and reduces soil erosion, to mention a few. Productive use of water resources should recognize these ecological services.

Regarding e-flow, while the fractions proposed by [76] are generic and can be applied to catchments of any size and in any physiographic conditions, it undermines the importance of emulating the natural flow regime with its seasonal variability, flow magnitude, frequency, event duration, and rise and fall of the hydrograph.

The lack of standardized processing and inclusion of HESS processes in river basin profiles prevents policymakers from realizing the value of water for provisioning and regulating services.

The methodology demonstrated by this paper proves that ecohydrological models are proper tools to quantify complex hydrological ecosystem services. Future works can focus on the fusion of ecohydrological models and remote sensing to provide a seamless zoom of HESS's spatial and temporal variation as well as stimulating policy impacts on nature and humans.

6. Conclusions

The principles of Integrated Water Resources Management (IWRM), conservation of natural capital, and water accounting require Hydrological Eco-System Services (HESS) to be determined. In this study, a number of HESS indicators were modeled for the Day River Basin in Vietnam using remote sensing and the SWAT model based on the definition of the framework initiated by CGIAR and IWMI's Water Land and Ecosystem Program. The spatial and temporal distribution of 11 HESS indicators quantified across the basin highlighted the provisioning and regulating character of our living environment in Southeast Asia. Geographical hotspots with lower and higher contribution could be identified, being a logical result of combinations of hydrological processes, climate, soil type, and the current land use.

These types of HESS assessments can be used by water resources planners in exploring multiple management scenarios and their implications for ecosystem services or "disservices." Think about reforestation, irrigation development, land consolidation, and urban

growth: a scenario analysis requires an eco-hydrological simulation model; this cannot be done by means of earth observations. Models such as SWAT host a wide suite of simulation options and can provide the data at a daily time step. The latter is required to cover dynamic processes such as peak flow attenuation and flood hazard. This feature was also highlighted by demonstrating the capabilities in HESS quantification by combining the use of SWAT and SWAT-CUP to model complex terrestrial eco-hydrological processes. Various biophysical processes were modeled in a spatial-temporal context to reveal interactions between ecosystems and benefits to humans.

A crucial step in achieving progress in eco-hydrological modeling is the inclusion of advanced earth observation data. With the arrival of many new algorithms, there are new technical opportunities to spatially calibrate specific eco-hydrologic processes. More future research on the integration of remote sensing data and eco-hydrological models should therefore be encouraged.

Author Contributions: L.T.H. and W.G.M.B. conceived and designed the experiments; L.T.H. performed the experiments; L.T.H. and W.G.M.B. analyzed the data; L.T.H. wrote the paper; W.G.M.B. revised the paper. All authors have read and agreed to the published version of the manuscript.

Funding: A workshop with international scientists was organized as part of a CGIAR Water, Land, and Ecosystems program, where many aspects of HESS were discussed. Support is also made available through the Vietnam Ministry of Science and Technology (MOST) (grant no. NDT/e-Asia/22/26). The authors would like to express our gratitude for this support.

Data Availability Statement: Please contact the author for data requests.

Acknowledgments: The authors express their gratitude towards five anonymous reviewers for their valuable comments to the manuscripts. The authors are thankful to Natalia Estrada-Carmona from the International Center for Tropical Agriculture (CIAT), Lisa Rebelo and Mathew McCartney from the International Water Management Institute (IWMI), Martine Rutten from TU Delft for the fruitful discussions on hydrological ecosystem services in the Mekong and Red River Delta.

Conflicts of Interest: The authors declare no conflict of interest.

Appendix A. Calculation of Intermediate Parameters for HESS Quantification

Horizontal Fast Overland Flow

Fast surface runoff in SWAT is calculated per unit of land using the common SCS curve number procedure [58]:

$$\boldsymbol{Q_{surf}} = \frac{(\boldsymbol{P} - \boldsymbol{I_a})^2}{(\boldsymbol{P} - \boldsymbol{I_a}+\boldsymbol{S})} \quad \text{(A1)}$$

where Q_{surf} is the surface runoff (mm/d) calculated on daily timestep, and P is the precipitation from rainfall and snowfall (mm/d). In the case of the Day Basin, precipitation is contributed by rainfall. I_a is the initial abstraction which includes surface storage and interception (mm/d), and S is an empirical retention parameter that reflects infiltration capacity and soil moisture deficit (mm/d). The retention parameter S varies spatially and depends on soil type, land use, the slope of the terrain, and soil moisture deficit.

$$\boldsymbol{S} = \mathbf{25.4}\left(\frac{\mathbf{1000}}{\boldsymbol{CN}} - \mathbf{10}\right) \quad \text{(A2)}$$

where CN is the Curve Number for the day (mm/d). Note that soil moisture content and S have to be dynamic [86]. SWAT defines three antecedent moisture conditions: dry (wilting point), average, and wet (field capacity), and will adjust S accordingly. This is an example of semi-dynamic water retention. The surface runoff computed in the context of HESS relates to rainfall and snowfall only.

Percolation

The equation used to calculate the amount of water that percolates to the layer underneath—without bypass in cracked soils—is:

$$w_{perc} = SW_{excess}\left\{1 - exp^{\left(-\frac{\Delta t}{TT_{perc}}\right)}\right\} \quad \text{(A3)}$$

where w_{perc} being the amount of water percolating to the underlying soil layer (mm H_2O), SW_{excess} is the drainable volume of water in the soil layer on a given day (mm), Δt is the length of the time step (d), and TT_{perc} is the travel time for percolation (d). The travel time can be computed as the ratio of the layer of water that percolates from the root zone and the value of the saturated hydraulic conductivity K_{sat}.

Lateral Groundwater Movement

The lateral groundwater flow Q_{lat} will be significant in areas with soils having high hydraulic conductivities in surface layers and an impermeable or semipermeable layer at a shallow depth. In such a system, rainfall will percolate vertically until it encounters the impermeable layer. The water then ponds above the impermeable layer, forming a saturated zone of water, i.e., a perched water table. This saturated zone is the source of water for lateral subsurface flow. The mathematical expression for Q_{lat} is based on Neitsch et al., 2011 [57]:

$$Q_{lat} = 0.024.\left(\frac{2.SW_{ly,excess}.K_{sat}.slp}{\varphi_d.L_{hill}}\right) \quad \text{(A4)}$$

where: $SW_{ly,excess}$ is the drainable volume of water stored in the saturated zone of the hillslope per unit area (mm/d), L_{hill} is the hillslope length (m), φ_d is the drainable porosity of the soil layer (mm/mm), K_{sat} is the saturated hydraulic conductivity (mm/h), and slp is the increase in elevation per unit distance. SWAT partitions groundwater into two aquifer systems: a shallow, unconfined aquifer which contributes return flow to streams within the watershed, and a deep, confined aquifer which contributes return flow to streams outside the watershed [33]. The outflow from the unconfined aquifer to the stream Q_{bf} is approximated as being a stationary drainage flow formulated according to the Hooghoudt drainage equation provided that the shallow aquifer exceeds a threshold value [87]:

$$Q_{gw} = \frac{8000\,K_{sat}}{L_{gw}^2}h_{wtbl} \quad \text{(A5)}$$

where Q_{gw} is the groundwater flow into the stream or river on day i (mm/d), K_{sat} is the hydraulic conductivity of the aquifer (mm/d), h_{wtbl} is the height of the water table (m), and L_{gw} is the distance between the HRU to the main channel (m).

Maximum Increase in Biomass

The maximum increase in biomass (ΔBio_max) on a given day that will result from the intercepted photosynthetically active radiation is estimated by [88] as:

$$\Delta Bio\_max = LUE.APAR \quad \text{(A6)}$$

where ΔBio_max is the potential increase in total plant biomass on a given day (g/m^2/d), LUE is the Light-use efficiency of the plant (g/MJ), and $APAR$ is the amount of Absorbed Photosynthetically Active Radiation on a given day (MJ m^{-2}). It is also known as net carbon assimilation because corrections for respiration have been applied already. The photosynthetic rate of a canopy is a linear function of radiant energy. $APAR$ can be calculated using Beer's formula:

$$APAR = 0.5.K\downarrow.[1 - exp(-k_l.LAI)] \quad \text{(A7)}$$

where $K\downarrow$ the global radiation incident to the land surface (MJ m^{-2}), k_l is the light extinction coefficient, and *LAI* is the leaf area index. The *LAI* development is strongly coupled to prevailing heat units and a number of plant species-dependent *LAI* values. *LAI* from the SWAT model was calibrated against *LAI* derived from MODIS 15 to derive plant physiology and plant growth as described in [46].

Heat Fluxes

Sensible heat flux (*H*) is calculated using the following formula:

$$\boldsymbol{H = Rn - LE} \qquad \left(\mathbf{W/m^2}\right) \tag{A8}$$

Latent heat flux (*LE*) is related to actual ET as follows:

$$\boldsymbol{LE = \rho_w L\, ET} \qquad \left(\mathbf{W/m^2}\right) \tag{A9}$$

with ρ_w being the density of water (kg/m^3), *L* is the latent heat of vaporization (J/kg), and ET is the water vapor flux expressed in m/s. The net radiation in SWAT is computed according to the suggestions of Doorenbos and Pruitt (1977) and Allen et al. (1998):

$$\boldsymbol{R_n = (1-\alpha)K_{\downarrow} - [0.9(1-cc)+0.1]\left[0.34 - 0.139\sqrt{e}\right]\sigma T^4} \left(\mathbf{W/m^2}\right) \tag{A10}$$

where α is the surface albedo, cc is cloud cover, e is the actual vapor pressure (mbar), σ is the Stefan Boltzmann constant ($W/m^2/K^4$), and T is the air temperature (K).

References

1. Millennium Ecosystem Assessment (Program). (Ed.) *Ecosystems and Human Well-Being: Wetlands and Water Synthesis: A Report of the Millennium Ecosystem Assessment*; World Resources Institute: Washington, DC, USA, 2005; ISBN 978-1-56973-597-8.
2. Brauman, K.A.; Daily, G.C.; Duarte, T.K.; Mooney, H.A. The Nature and Value of Ecosystem Services: An Overview Highlighting Hydrologic Services. *Annu. Rev. Environ. Resour.* **2007**, *32*, 67–98. [CrossRef]
3. Chapin, F.S.; Matson, P.A.; Mooney, H.A. *Principles of Terrestrial Ecosystem Ecology*; Springer: New York, NY, USA, 2002; ISBN 978-0-387-95439-4.
4. Holland, R.A.; Darwall, W.R.T.; Smith, K.G. Conservation Priorities for Freshwater Biodiversity: The Key Biodiversity Area Approach Refined and Tested for Continental Africa. *Biol. Conserv.* **2012**, *148*, 167–179. [CrossRef]
5. Brauman, K.A. Hydrologic Ecosystem Services: Linking Ecohydrologic Processes to Human Well-being in Water Research and Watershed Management. *WIREs Water* **2015**, *2*, 345–358. [CrossRef]
6. Hoekstra, A.Y.; Mekonnen, M.M. The Water Footprint of Humanity. *Proc. Natl. Acad. Sci. USA* **2012**, *109*, 3232–3237. [CrossRef] [PubMed]
7. FAO. *AQUASTAT FAO's Information System on Water and Agriculture*; FAO: Rome, Italy, 2021.
8. Hansen, R.; Frantzeskaki, N.; McPhearson, T.; Rall, E.; Kabisch, N.; Kaczorowska, A.; Kain, J.-H.; Artmann, M.; Pauleit, S. The Uptake of the Ecosystem Services Concept in Planning Discourses of European and American Cities. *Ecosyst. Serv.* **2015**, *12*, 228–246. [CrossRef]
9. Harrison-Atlas, D.; Theobald, D.M.; Goldstein, J.H. A Systematic Review of Approaches to Quantify Hydrologic Ecosystem Services to Inform Decision-Making. *Int. J. Biodivers. Sci. Ecosyst. Serv. Manag.* **2016**, *12*, 160–171. [CrossRef]
10. Grizzetti, B.; Lanzanova, D.; Liquete, C.; Reynaud, A.; Cardoso, A.C. Assessing Water Ecosystem Services for Water Resource Management. *Environ. Sci. Policy* **2016**, *61*, 194–203. [CrossRef]
11. CGIAR Research Program on Water, Land and Ecosystems (WLE). *Ecosystem Services and Resilience Framework*; International Water Management Institute (IWMI), CGIAR Research Program on Water, Land and Ecosystems (WLE): Colombo, Sri Lanka, 2014.
12. Ha, L.T.; Bastiaanssen, W.G.M.; Simons, G.W.H.; Poortinga, A. A New Framework of 17 Hydrological Ecosystem Services (HESS17) for Supporting River Basin Planning and Environmental Monitoring. *Sustainability* **2023**, *15*, 6182. [CrossRef]
13. Karimi, P.; Bastiaanssen, W.G.M.; Molden, D. Water Accounting Plus (WA+)—A Water Accounting Procedure for Complex River Basins Based on Satellite Measurements. *Hydrol. Earth Syst. Sci.* **2013**, *17*, 2459–2472. [CrossRef]
14. Bastiaanssen, W.; Karimi, P.; Rebelo, L.-M.; Duan, Z.; Senay, G.; Muttuwatte, L.; Smakhtin, V. Earth Observation Based Assessment of the Water Production and Water Consumption of Nile Basin Agro-Ecosystems. *Remote Sens.* **2014**, *6*, 10306–10334. [CrossRef]
15. Pereira, P. Ecosystem Services in a Changing Environment. *Sci. Total Environ.* **2020**, *702*, 135008. [CrossRef]
16. Le Maitre, D.C.; Milton, S.J.; Jarmain, C.; Colvin, C.A.; Saayman, I.; Vlok, J.H. Linking Ecosystem Services and Water Resources: Landscape-Scale Hydrology of the Little Karoo. *Front. Ecol. Environ.* **2007**, *5*, 261–270. [CrossRef]

17. Eigenbrod, F.; Armsworth, P.R.; Anderson, B.J.; Heinemeyer, A.; Gillings, S.; Roy, D.B.; Thomas, C.D.; Gaston, K.J. The Impact of Proxy-Based Methods on Mapping the Distribution of Ecosystem Services. *J. Appl. Ecol.* **2010**, *47*, 377–385. [CrossRef]
18. European Commission. *Directorate General for the Environment. Mapping and Assessment of Ecosystems and Their Services: Indicators for Ecosystem Assessments under Action 5 of the EU Biodiversity Strategy to 2020: 2nd Report—Final, February 2014*; Publications Office: Luxembourg, 2014.
19. Leh, M.D.K.; Matlock, M.D.; Cummings, E.C.; Nalley, L.L. Quantifying and Mapping Multiple Ecosystem Services Change in West Africa. *Agric. Ecosyst. Environ.* **2013**, *165*, 6–18. [CrossRef]
20. Pearson, T.R.H.; Brown, S.L.; Birdsey, R.A. *Measurement Guidelines for the Sequestration of Forest Carbon*; U.S. Department of Agriculture, Forest Service, Northern Research Station: Newtown Square, PA, USA, 2007; 42p. [CrossRef]
21. Saatchi, S.S.; Harris, N.L.; Brown, S.; Lefsky, M.; Mitchard, E.T.A.; Salas, W.; Zutta, B.R.; Buermann, W.; Lewis, S.L.; Hagen, S.; et al. Benchmark Map of Forest Carbon Stocks in Tropical Regions across Three Continents. *Proc. Natl. Acad. Sci. USA* **2011**, *108*, 9899–9904. [CrossRef]
22. Kumar, P.; Economics of Ecosystems and Biodiversity (Project) (Eds.) *The Economics of Ecosystems and Biodiversity: Ecological and Economic Foundations*; Earthscan: London, UK; Washington, DC, USA, 2010; ISBN 978-1-84971-212-5.
23. Skidmore, A.K.; Pettorelli, N.; Coops, N.C.; Geller, G.N.; Hansen, M.; Lucas, R.; Mücher, C.A.; O'Connor, B.; Paganini, M.; Pereira, H.M.; et al. Environmental Science: Agree on Biodiversity Metrics to Track from Space. *Nature* **2015**, *523*, 403–405. [CrossRef]
24. Saad, R.; Koellner, T.; Margni, M. Land Use Impacts on Freshwater Regulation, Erosion Regulation, and Water Purification: A Spatial Approach for a Global Scale Level. *Int. J. Life Cycle Assess.* **2013**, *18*, 1253–1264. [CrossRef]
25. Simons, G.; Bastiaanssen, W.; Ngô, L.; Hain, C.; Anderson, M.; Senay, G. Integrating Global Satellite-Derived Data Products as a Pre-Analysis for Hydrological Modelling Studies: A Case Study for the Red River Basin. *Remote Sens.* **2016**, *8*, 279. [CrossRef]
26. Milne, R.; Brown, T.A. Carbon in the Vegetation and Soils of Great Britain. *J. Environ. Manag.* **1997**, *49*, 413–433. [CrossRef]
27. McGuire, A.D.; Christensen, T.R.; Hayes, D.; Heroult, A.; Euskirchen, E.; Kimball, J.S.; Koven, C.; Lafleur, P.; Miller, P.A.; Oechel, W.; et al. An Assessment of the Carbon Balance of Arctic Tundra: Comparisons among Observations, Process Models, and Atmospheric Inversions. *Biogeosciences* **2012**, *9*, 3185–3204. [CrossRef]
28. Kiptala, J.; Mul, M.; Mohamed, Y.; Bastiaanssen, W.; van der Zaag, P. Mapping Ecological Production and Benefits from Water Consumed in Agricultural and Natural Landscapes: A Case Study of the Pangani Basin. *Remote Sens.* **2018**, *10*, 1802. [CrossRef]
29. Francesconi, W.; Srinivasan, R.; Pérez-Miñana, E.; Willcock, S.P.; Quintero, M. Using the Soil and Water Assessment Tool (SWAT) to Model Ecosystem Services: A Systematic Review. *J. Hydrol.* **2016**, *535*, 625–636. [CrossRef]
30. Angerer, J.P. 16. Technologies, Tools and Methodologies for Forage Evaluation in Grasslands and Rangelands. In *National Feed Assessments*; FAO: Quebec City, QC, Canada, 2012; pp. 165–200.
31. Awan, U.K.; Ismaeel, A. A New Technique to Map Groundwater Recharge in Irrigated Areas Using a SWAT Model under Changing Climate. *J. Hydrol.* **2014**, *519*, 1368–1382. [CrossRef]
32. Schulp, C.J.E.; Alkemade, R.; Klein Goldewijk, K.; Petz, K. Mapping Ecosystem Functions and Services in Eastern Europe Using Global-Scale Data Sets. *Int. J. Biodivers. Sci. Ecosyst. Serv. Manag.* **2012**, *8*, 156–168. [CrossRef]
33. Arnold, J.G.; Srinivasan, R.; Muttiah, R.S.; Williams, J.R. Large area hydrologic modeling and assessment part i: Model development. *J. Am. Water Resour. Assoc.* **1998**, *34*, 73–89. [CrossRef]
34. Villa, F.; Athanasiadis, I.N.; Rizzoli, A.E. Modelling with Knowledge: A Review of Emerging Semantic Approaches to Environmental Modelling. *Environ. Model. Softw.* **2009**, *24*, 577–587. [CrossRef]
35. Vigerstol, K.L.; Aukema, J.E. A Comparison of Tools for Modeling Freshwater Ecosystem Services. *J. Environ. Manag.* **2011**, *92*, 2403–2409. [CrossRef]
36. Tallis, H.; Polasky, S. Mapping and Valuing Ecosystem Services as an Approach for Conservation and Natural-Resource Management. *Ann. N. Y. Acad. Sci.* **2009**, *1162*, 265–283. [CrossRef]
37. Liang, X.; Lettenmaier, D.P.; Wood, E.F.; Burges, S.J. A Simple Hydrologically Based Model of Land Surface Water and Energy Fluxes for General Circulation Models. *J. Geophys. Res.* **1994**, *99*, 14415. [CrossRef]
38. Dechmi, F.; Burguete, J.; Skhiri, A. SWAT Application in Intensive Irrigation Systems: Model Modification, Calibration and Validation. *J. Hydrol.* **2012**, *470–471*, 227–238. [CrossRef]
39. Van Griensven, A.; Ndomba, P.; Yalew, S.; Kilonzo, F. Critical Review of SWAT Applications in the Upper Nile Basin Countries. *Hydrol. Earth Syst. Sci.* **2012**, *16*, 3371–3381. [CrossRef]
40. Abbaspour, K.C.; Rouholahnejad, E.; Vaghefi, S.; Srinivasan, R.; Yang, H.; Kløve, B. A Continental-Scale Hydrology and Water Quality Model for Europe: Calibration and Uncertainty of a High-Resolution Large-Scale SWAT Model. *J. Hydrol.* **2015**, *524*, 733–752. [CrossRef]
41. Jayakrishnan, R.; Srinivasan, R.; Santhi, C.; Arnold, J.G. Advances in the Application of the SWAT Model for Water Resources Management. *Hydrol. Process.* **2005**, *19*, 749–762. [CrossRef]
42. Luo, Y.; He, C.; Sophocleous, M.; Yin, Z.; Hongrui, R.; Ouyang, Z. Assessment of Crop Growth and Soil Water Modules in SWAT2000 Using Extensive Field Experiment Data in an Irrigation District of the Yellow River Basin. *J. Hydrol.* **2008**, *352*, 139–156. [CrossRef]
43. Yang, Q.; Zhang, X. Improving SWAT for Simulating Water and Carbon Fluxes of Forest Ecosystems. *Sci. Total Environ.* **2016**, *569–570*, 1478–1488. [CrossRef]

44. Radcliffe, D.E.; Reid, D.K.; Blombäck, K.; Bolster, C.H.; Collick, A.S.; Easton, Z.M.; Francesconi, W.; Fuka, D.R.; Johnsson, H.; King, K.; et al. Applicability of Models to Predict Phosphorus Losses in Drained Fields: A Review. *J. Environ. Qual.* **2015**, *44*, 614–628. [CrossRef]
45. Krysanova, V.; White, M. Advances in Water Resources Assessment with SWAT—An Overview. *Hydrol. Sci. J.* **2015**, *60*, 771–783. [CrossRef]
46. Ha, L.T.; Bastiaanssen, W.G.M.; Van Griensven, A.; Van Dijk, A.I.J.M.; Senay, G.B. Calibration of Spatially Distributed Hydrological Processes and Model Parameters in SWAT Using Remote Sensing Data and an Auto-Calibration Procedure: A Case Study in a Vietnamese River Basin. *Water* **2018**, *10*, 212. [CrossRef]
47. Paca, V.H.d.M.; Espinoza-Dávalos, G.E.; Hessels, T.M.; Moreira, D.M.; Comair, G.F.; Bastiaanssen, W.G.M. The Spatial Variability of Actual Evapotranspiration across the Amazon River Basin Based on Remote Sensing Products Validated with Flux Towers. *Ecol. Process.* **2019**, *8*, 6. [CrossRef]
48. Sriwongsitanon, N.; Suwawong, T.; Thianpopirug, S.; Williams, J.; Jia, L.; Bastiaanssen, W. Validation of Seven Global Remotely Sensed ET Products across Thailand Using Water Balance Measurements and Land Use Classifications. *J. Hydrol. Reg. Stud.* **2020**, *30*, 100709. [CrossRef]
49. Farr, T.G.; Rosen, P.A.; Caro, E.; Crippen, R.; Duren, R.; Hensley, R.; Kobrick, M.; Paller, M.; Rodriguez, E.; Roth, L.; et al. The Shuttle Radar Topography Mission. *Rev. Geophys.* **2007**, *45*, RG2004. [CrossRef]
50. Bontemps, S.; Defourny, P.; van Bogaert, E.; Herold, M.; Kooistra, L.; Kalogirou, V.; Arino, O. Producing Global Land Cover Maps Consistent over Time to Respond the Needs of the Climate Modelling Community. In Proceedings of the 6th International Workshop on the Analysis of Multi-temporal Remote Sensing Images (Multi-Temp), Trento, Italy, 12–14 July 2011; pp. 161–164.
51. Rodell, M.; Houser, P.R.; Jambor, U.; Gottschalck, J.; Mitchell, K.; Meng, C.-J.; Arsenault, K.; Cosgrove, B.; Radakovich, J.; Bosilovich, M.; et al. The Global Land Data Assimilation System. *Bull. Am. Meteorol. Soc.* **2004**, *85*, 381–394. [CrossRef]
52. Myneni, R.; Knyazikhin, Y.; Park, T. MOD15A2H MODIS Leaf Area Index/FPAR 8-Day L4 Global 500m SIN Grid V006. NASA EOSDIS Land Processes DAAC. 2015. Available online: https://lpdaac.usgs.gov/products/mcd15a2hv006/ (accessed on 22 March 2023).
53. Nietsch, S.L.; Arnold, J.G.; Kiniry, J.R.; Srinivasan, R.; Williams, J.R. *SWAT: Soil and Water Assessment Tool User's Manual*; Texas Water Resources Institute, USDA Agricultural Research Service: College Station, TX, USA, 2002.
54. Arnold, J.G.; Moriasi, D.N.; Gassman, P.W.; Abbaspour, K.C.; White, M.J.; Srinivasan, R.; Santhi, C.; Harmel, R.D.; Van Griensven, A.; Van Liew, M.W.; et al. SWAT: Model Use, Calibration, and Validation. *Trans. ASABE* **2012**, *55*, 1491–1508. [CrossRef]
55. Immerzeel, W.W.; Droogers, P. Calibration of a Distributed Hydrological Model Based on Satellite Evapotranspiration. *J. Hydrol.* **2008**, *349*, 411–424. [CrossRef]
56. Strauch, M.; Volk, M. SWAT Plant Growth Modification for Improved Modeling of Perennial Vegetation in the Tropics. *Ecol. Model.* **2013**, *269*, 98–112. [CrossRef]
57. Neitsch, S.; Arnold, J.; Kiniry, J.; Williams, J.R. Soil and Water Asessment Tool Theoritical Documentation Version 2009. Texas Water Resources Institute Technical: College Station, TX, USA, 2011.
58. Soil Conservation Service U.S.S.C. *SCS National Engineering Handbook, Section 4: Hydrology*; Department of Agriculture: Washington, DC, USA, 1972; 762p.
59. Herrero, M.; Havlik, P.; Valin, H.; Notenbaert, A.; Rufino, M.C.; Thornton, P.K.; Blummel, M.; Weiss, F.; Grace, D.; Obersteiner, M. Biomass Use, Production, Feed Efficiencies, and Greenhouse Gas Emissions from Global Livestock Systems. *Proc. Natl. Acad. Sci. USA* **2013**, *110*, 20888–20893. [CrossRef]
60. Sassen, M.; Sheil, D.; Giller, K.E. Fuelwood Collection and Its Impacts on a Protected Tropical Mountain Forest in Uganda. *For. Ecol. Manag.* **2015**, *354*, 56–67. [CrossRef]
61. Ponce-Hernandez, R.; Koohafkan, P.; Antoine, J. *Assessing Carbon Stocks and Modelling Win-Win Scenarios of Carbon Sequestration through Land-Use Changes*; Food and Agriculture Organization: Roma, Italy, 2004.
62. Ahmad, M.-D.; Bastiaanssen, W.G.M. Retrieving Soil Moisture Storage in the Unsaturated Zone Using Satellite Imagery and Bi-Annual Phreatic Surface Fluctuations. *Irrig. Drain. Syst.* **2003**, *17*, 141–161. [CrossRef]
63. Savenije, H.H.G. The Runoff Coefficient as the Key to Moisture Recycling. *J. Hydrol.* **1996**, *176*, 219–225. [CrossRef]
64. Keys, P.W.; Wang-Erlandsson, L.; Gordon, L.J. Revealing Invisible Water: Moisture Recycling as an Ecosystem Service. *PLoS ONE* **2016**, *11*, e0151993. [CrossRef]
65. Van der Ent, R.J.; Savenije, H.H.G.; Schaefli, B.; Steele-Dunne, S.C. Origin and Fate of Atmospheric Moisture over Continents: Origin and Fate of Atmospheric Moisture Over Continents. *Water Resour. Res.* **2010**, *46*, W09525. [CrossRef]
66. Coerver, B. Regional Precipitation and Evaporation Patterns in South East Asia Based on ERA5 Data (Internal Note) 2007.
67. Eggleston, H.S.; Buendia, L.; Miwa, K.; Ngara, T.; Tanabe,, K. 2006 IPCC Guidelines for National Greenhouse Gas Inventories. In Proceedings of the Third Authors/Experts Meeting: Industrial Processes and Product Use, Washington, DC, USA, 27–29 July 2006.
68. Trischler, J.; Sandberg, D.; Thörnqvist, T. Estimating the Annual Above-Ground Biomass Production of Various Species on Sites in Sweden on the Basis of Individual Climate and Productivity Values. *Forests* **2014**, *5*, 2521–2541. [CrossRef]
69. Vleeshouwers, L.M.; Verhagen, A. Carbon Emission and Sequestration by Agricultural Land Use: A Model Study for Europe: Carbon Sequestration by European Agriculture. *Glob. Chang. Biol.* **2002**, *8*, 519–530. [CrossRef]
70. Yoshida, S. *Fundamentals of Rice Crop Science*; International Rice Research Institute: Los Baños, Philippines, 1981; Volume 279, pp. 252–267.

71. Duan, Z.; Bastiaanssen, W.G.M. Evaluation of Three Energy Balance-Based Evaporation Models for Estimating Monthly Evaporation for Five Lakes Using Derived Heat Storage Changes from a Hysteresis Model. *Environ. Res. Lett.* **2017**, *12*, 024005. [CrossRef]
72. Klok, L.; Zwart, S.; Verhagen, H.; Mauri, E. The Surface Heat Island of Rotterdam and Its Relationship with Urban Surface Characteristics. *Resour. Conserv. Recycl.* **2012**, *64*, 23–29. [CrossRef]
73. Senay, G.B.; Bohms, S.; Singh, R.K.; Gowda, P.H.; Velpuri, N.M.; Alemu, H.; Verdin, J.P. Operational Evapotranspiration Mapping Using Remote Sensing and Weather Datasets: A New Parameterization for the SSEB Approach. *JAWRA J. Am. Water Resour. Assoc.* **2013**, *49*, 577–591. [CrossRef]
74. Mohamed, Y.A.; Bastiaanssen, W.G.M.; Savenije, H.H.G. Spatial Variability of Evaporation and Moisture Storage in the Swamps of the Upper Nile Studied by Remote Sensing Techniques. *J. Hydrol.* **2004**, *289*, 145–164. [CrossRef]
75. Smakhtin, V.; Revenga, C.; Döll, P. A Pilot Global Assessment of Environmental Water Requirements and Scarcity. *Water Int.* **2004**, *29*, 307–317. [CrossRef]
76. Smakhtin, V.; Eriyagama, N. Developing a Software Package for Global Desktop Assessment of Environmental Flows. *Environ. Model. Softw.* **2008**, *23*, 1396–1406. [CrossRef]
77. Tuinenburg, O.A.; Hutjes, R.W.A.; Stacke, T.; Wiltshire, A.; Lucas-Picher, P. Effects of Irrigation in India on the Atmospheric Water Budget. *J. Hydrometeorol.* **2014**, *15*, 1028–1050. [CrossRef]
78. Iroumé, A.; Mayen, O.; Huber, A. Runoff and Peak Flow Responses to Timber Harvest and Forest Age in Southern Chile. *Hydrol. Process.* **2006**, *20*, 37–50. [CrossRef]
79. Simons, G.; Poortinga, A.; Bastiaanssen, W.G.M.; Saah, D.S.; Troy, D.; Hunink, J.E.; de Klerk, M.; Rutten, M.; Cutter, P.; Rebelo, L.-M.; et al. *On Spatially Distributed Hydrological Ecosystem Services: Bridging the Quantitative Information Gap Using Remote Sensing and Hydrological Models*; White paper; FutureWater: Wageningen, The Netherlands, 2017.
80. Gaur, S. *Distributed Hydrological Modelling Under Climate Change: A Way-Forward For Accounting, Planning and Management of Water Resources*; IIT Kharagpur: Kharagpur, India, 2022.
81. Gaur, S.; Singh, B.; Bandyopadhyay, A.; Stisen, S.; Singh, R. Spatial Pattern-based Performance Evaluation and Uncertainty Analysis of a Distributed Hydrological Model. *Hydrol. Process.* **2022**, *36*, e14586. [CrossRef]
82. Terrado, M.; Acuña, V.; Ennaanay, D.; Tallis, H.; Sabater, S. Impact of Climate Extremes on Hydrological Ecosystem Services in a Heavily Humanized Mediterranean Basin. *Ecol. Indic.* **2014**, *37*, 199–209. [CrossRef]
83. Molden, D. *Accounting for Water Use and Productivity*; IWMI: Ruhunupura, Sri Lanka, 1997.
84. Molden, D.; Sakthivadivel, R. Water Accounting to Assess Use and Productivity of Water. *Int. J. Water Resour. Dev.* **1999**, *15*, 55–71. [CrossRef]
85. Hellegers, P.J.G.J.; Soppe, R.; Perry, C.J.; Bastiaanssen, W.G.M. Combining Remote Sensing and Economic Analysis to Support Decisions That Affect Water Productivity. *Irrig. Sci.* **2009**, *27*, 243–251. [CrossRef]
86. Choudhury, B.J.; DiGirolamo, N.E. A Biophysical Process-Based Estimate of Global Land Surface Evaporation Using Satellite and Ancillary Data I. Model Description and Comparison with Observations. *J. Hydrol.* **1998**, *205*, 164–185. [CrossRef]
87. Ritzema, H. (Ed.) Subsurface Flow to D Subsurface flows to drains. In *Drainage Principles and Applications*; ILRI Publication: Wageningen, The Netherlands, 1994; pp. 283–294.rains.
88. Monteith, J.L. Climate and the Efficiency of Crop Production in Britain. *Philos. Trans. R. Soc. Lond. B Biol. Sci.* **1977**, *281*, 277–294. [CrossRef]